

TNF and IL-1 exhibit distinct ubiquitin requirements for inducing NEMO-IKK supramolecular structures.

Nadine Tarantino, Jean-Yves Tinevez, Elizabeth Faris Crowell, Bertrand Boisson, Ricardo Henriques, Musa Mhlanga, Fabrice Agou, Alain Israël, Emmanuel Laplantine

▶ **To cite this version:**

Nadine Tarantino, Jean-Yves Tinevez, Elizabeth Faris Crowell, Bertrand Boisson, Ricardo Henriques, et al.. TNF and IL-1 exhibit distinct ubiquitin requirements for inducing NEMO-IKK supramolecular structures.. Journal of Cell Biology, 2014, 204 (2), pp.231-45. 10.1083/jcb.201307172 . pasteur-01539965

HAL Id: pasteur-01539965
https://pasteur.hal.science/pasteur-01539965

Submitted on 15 Jun 2017

HAL is a multi-disciplinary open access archive for the deposit and dissemination of scientific research documents, whether they are published or not. The documents may come from teaching and research institutions in France or abroad, or from public or private research centers.

L'archive ouverte pluridisciplinaire **HAL**, est destinée au dépôt et à la diffusion de documents scientifiques de niveau recherche, publiés ou non, émanant des établissements d'enseignement et de recherche français ou étrangers, des laboratoires publics ou privés.



Distributed under a Creative Commons Attribution - NonCommercial - ShareAlike 4.0 International License

Published January 20, 2014

TNF and IL-1 exhibit distinct ubiquitin requirements for inducing NEMO–IKK supramolecular structures

Nadine Tarantino,[1] Jean-Yves Tinevez,[3] Elizabeth Faris Crowell,[2] Bertrand Boisson,[5] Ricardo Henriques,[4,6,7] Musa Mhlanga,[6,8] Fabrice Agou,[1] Alain Israël,[1] and Emmanuel Laplantine[1]

[1]Unité de Signalisation Moléculaire et Activation Cellulaire and [2]Laboratoire Trafic Membranaire et Division Cellulaire, Institut Pasteur, Centre National de la Recherche Scientifique URA 2582, Paris 75015, France
[3]Plateforme d'Imagerie Dynamique and [4]Computational Imaging and Modeling Group, Institut Pasteur, Paris 75015, France
[5]St. Giles Laboratory of Human Genetics of Infectious Diseases, Rockefeller Branch, The Rockefeller University, New York, NY 10065
[6]Gene Expression and Biophysics Unit, Instituto de Medicina Molecular, Faculdade de Medicina Universidade de Lisboa, Lisboa, 1649-028 Portugal
[7]Medical Research Council Laboratory for Molecular Cell Biology, University College London, London WC1E 6BT, England, UK
[8]Gene Expression and Biophysics Group, Synthetic Biology Emerging Research Area, Biosciences Unit, Council for Scientific and Industrial Research, Pretoria, Gauteng 0001, South Africa

Nuclear factor κB (NF-κB) essential modulator (NEMO), a regulatory component of the IκB kinase (IKK) complex, controls NF-κB activation through its interaction with ubiquitin chains. We show here that stimulation with interleukin-1 (IL-1) and TNF induces a rapid and transient recruitment of NEMO into punctate structures that are anchored at the cell periphery. These structures are enriched in activated IKK kinases and ubiquitinated NEMO molecules, which suggests that they serve as organizing centers for the activation of NF-κB. These NEMO-containing structures colocalize with activated TNF receptors but not with activated IL-1 receptors. We investigated the involvement of nondegradative ubiquitination in the formation of these structures, using cells deficient in K63 ubiquitin chains or linear ubiquitin chain assembly complex (LUBAC)-mediated linear ubiquitination. Our results indicate that, unlike TNF, IL-1 requires K63-linked and linear ubiquitin chains to recruit NEMO into higher-order complexes. Thus, different mechanisms are involved in the recruitment of NEMO into supramolecular complexes, which appear to be essential for NF-κB activation.

Introduction

The nuclear factor κB (NF-κB) family of transcription factors plays a critical role in a large number of normal and pathological processes, such as immune and inflammatory responses, developmental processes, cellular growth, and apoptosis (for review see Hayden and Ghosh, 2012). In resting cells, NF-κB is kept inactive in the cytoplasm by direct interaction with inhibitor of NF-κB (IκB) inhibitory proteins. In response to diverse signals, a cytosolic kinase complex known as the IκB kinase (IKK) complex is activated, leading to the phosphorylation of the IκBs, which are consequently ubiquitinated and degraded by the 26 S proteasome. This leads to the nuclear translocation of NF-κB, which then activates its target genes. The activation of the IKK complex is therefore believed to constitute a key event in NF-κB signal transduction in response to many stimuli. This complex consists of two kinase subunits—IKKα and IKKβ—and a regulatory subunit, NF-κB essential modulator (NEMO; also known as IKKγ). NEMO has no enzyme activity, but is absolutely required for activation of the IKK kinases in the canonical NF-κB pathway. An alternative pathway that does not require NEMO but depends on the kinases IKKα and NIK also leads to NF-κB activation (Sun, 2011).

Our understanding of the biochemical mechanism underlying the essential signaling function of NEMO has increased considerably over the last decade, through the discovery of mutations in the NEMO gene leading to mild to severe human disease affecting essentially, but not exclusively, the immune system (Courtois and Israël, 2011). The mutations identified are

Correspondence to Emmanuel Laplantine: emmanuel.laplantine@pasteur.fr

Abbreviations used in this paper: Dox, doxycycline; HOIL1, heme-oxidized IRP2 ubiquitin ligase 1; IκB, inhibitor of NF-κB; IKK, IκB kinase; IL-1, interleukin-1; IL-1R, IL-1 receptor; IRAK1, IL-1R–associated kinase 1; LPS, lipopolysaccharides; LUBAC, linear ubiquitin chain assembly complex; MSD, mean square displacement; NEMO, NF-κB essential modulator; NF-κB, nuclear factor κB; RSC, receptor signaling complex; TIRF, total internal reflection fluorescence; vOTU, viral ovarian tumor domain.

© 2014 Tarantino et al. This article is distributed under the terms of an Attribution–Noncommercial–Share Alike–No Mirror Sites license for the first six months after the publication date (see http://www.rupress.org/terms). After six months it is available under a Creative Commons License (Attribution–Noncommercial–Share Alike 3.0 Unported license, as described at http://creativecommons.org/licenses/by-nc-sa/3.0/).

Supplemental Material can be found at:
/content/suppl/2014/01/16/jcb.201307172.DC1.html

The Rockefeller University Press $30.00
J. Cell Biol. Vol. 204 No. 2 231–245
www.jcb.org/cgi/doi/10.1083/jcb.201307172

THE JOURNAL OF CELL BIOLOGY

Downloaded from on June 15, 2017

Published January 20, 2014

dispersed throughout the NEMO gene, but several point mutations affecting the C-terminal half of NEMO have revealed that this region contains two ubiquitin-binding domains, a so-called UBAN/NOA domain and a ubiquitin-binding zinc-finger (ZF) domain, both of which are critical for NEMO activity. These domains allow NEMO to interact with different types of polyubiquitin chains. The NOA domain of NEMO is necessary and sufficient for the binding of linear ubiquitin chains (Lo et al., 2009; Rahighi et al., 2009), but both the NOA and ZF are required for the binding of K63-linked ubiquitin chains (Laplantine et al., 2009).

Unlike K48 ubiquitination, which targets substrates for proteasomal degradation, K63-linked and, more recently, linear ubiquitination have been shown to be important for NF-κB activation by providing a recruitment platform and signaling cues (Chen, 2012; Iwai, 2012). K63-linked ubiquitination was the first nondegradative ubiquitination event shown to play a role in NF-κB signal transduction (Deng et al., 2000). These types of ubiquitin chains are formed by E3-ubiquitin ligases that differ depending on the stimulus. In the TNF pathway, E3-ligases belonging to the TRAF and cIAP families are responsible for the K63-linked ubiquitination of the TNF receptor–interacting protein RIP1 (for review see Chen, 2012). K63-ubiquitinated RIP1 is believed to be responsible for the recruitment of the IKK complex via NEMO (Wu et al., 2006). In the interleukin-1 (IL-1) pathway, TRAF6, and the E3-ligase Pellino are responsible for the K63-linked ubiquitination of IL-1 receptor (IL-1R)–associated kinase 1 (IRAK1), a kinase recruited to the IL-1R. As for RIP1 in the TNF pathway, it has been suggested that the attachment of K63-linked ubiquitin chains to IRAK1 leads to recruitment of the NEMO–IKK complex (Conze et al., 2008; Ordureau et al., 2008; Windheim et al., 2008). K63-linked ubiquitination events occur in response to both TNF and IL-1, but the requirement of these events for the activation of NF-κB may differ between stimuli. Indeed, it has been reported that the K63-specific ubiquitin-conjugating enzyme Ubc13 is required for IL-1–induced but not for TNF-induced IKK activation (Deng et al., 2000; Yamamoto et al., 2006; Xu et al., 2009). Moreover, it has been shown, using a ubiquitin replacement strategy (Xu et al., 2009), that K63-linked ubiquitin chains are indispensable for the induction of NF-κB activation by IL-1, but not by TNF. Thus, although K63-linked ubiquitin chains play essential roles in signaling and, possibly, in IL-1–induced NF-κB activation, they may not be absolutely required in response to other stimuli, such as TNF.

Linear polyubiquitin chains consist of ubiquitin molecules covalently linked through the C-terminal glycine of a ubiquitin molecule and the N-terminal methionine of the ubiquitin molecule preceding it in the chain. A unique E3-ligase complex able to generate this type of ubiquitin modification, known as linear ubiquitin chain assembly complex (LUBAC), has been shown to play a role in NF-κB signaling (Kirisako et al., 2006; Tokunaga et al., 2009; Haas et al., 2009). LUBAC is a ternary complex composed of HOIP (the catalytic subunit), heme-oxidized IRP2 ubiquitin ligase 1 (HOIL1), and SHARPIN (Iwai, 2012). TNF-induced NF-κB activation is reduced in cells depleted of LUBAC components by RNAi and in HOIL1$^{-/-}$ MEF cells (Haas et al., 2009; Tokunaga et al., 2009). LUBAC has been shown to be a functional component of the native TNF receptor signaling complex (RSC; Haas et al., 2009). We recently identified loss-of-function mutations of the gene encoding the LUBAC component HOIL1 in humans. These mutations lead to severe immunodeficiency and autoinflammation, providing a link between LUBAC and human physiology (Boisson et al., 2012). We found that fibroblasts isolated from HOIL-deficient patients displayed very low levels of NF-κB activation in response to IL-1, whereas the TNF response was only slightly impaired. These findings indicate that LUBAC-mediated linear ubiquitination may be required to different extents for NF-κB activation in response to IL-1 and TNF.

In resting cells, the NEMO–IKK complex resides in the cytosol, and stimulation is thought to lead to its recruitment to specific multiprotein complexes, although the composition and subcellular distribution of these complexes have not yet been clearly defined. In this study, we show that the stimulation of cells with two different proinflammatory cytokines—IL-1 and TNF—induces the local and transient recruitment of NEMO and activated IKK kinases into small punctate structures. Moreover, this event is fully correlated with transduction of the downstream NF-κB signal. We also show here that the requirement for K63-linked and linear ubiquitination differs between the responses to TNF and IL-1: neither of these ubiquitin modifications appears to be required separately to induce the relocalization of NEMO in response to TNF, whereas both types of ubiquitination are critical for inducing the recruitment of NEMO to punctate structures in response to IL-1.

Results

NEMO concentrates in punctate structures in response to cytokine stimulation

We investigated whether cytokine stimulation induced a redistribution of NEMO in the cell by first determining the change in the subcellular distribution of NEMO after stimulation with IL-1, by immunofluorescence. NEMO underwent a striking relocalization into small punctate structures after IL-1 treatment (Fig. 1 A). The local accumulation of NEMO in small foci induced by IL-1 was more clearly observed if the cells were treated with saponin before fixation (Fig. 1 A, right). This treatment probably extracts cytosolic/soluble NEMO without affecting IL-1–induced NEMO-containing structures. In contrast to what was observed for IL-1 stimulation, no NEMO-containing punctae were observed after treatment with TNF alone (not depicted); instead, such punctae were observed only if the cells were treated with saponin before fixation (Fig. 1 B). We investigated whether NEMO-containing structures also contained the activated IKK kinases by performing immunofluorescence studies with an antibody recognizing phosphorylated (and therefore activated) IKKα and IKKβ. No signal was detected for phospho-IKKs (p-IKK) in untreated cells, whereas treatment with IL-1 or TNF led to a strong accumulation of p-IKK colocalizing with NEMO into foci (Fig. 2 A). Quantitative analyses of the colocalization of NEMO and p-IKK during a time course of IL-1 and TNF stimulation (Fig. 2, B and C, respectively) revealed that the formation kinetics for NEMO-containing foci and for p-IKK–containing foci were similar.

Downloaded from on June 15, 2017

Published January 20, 2014

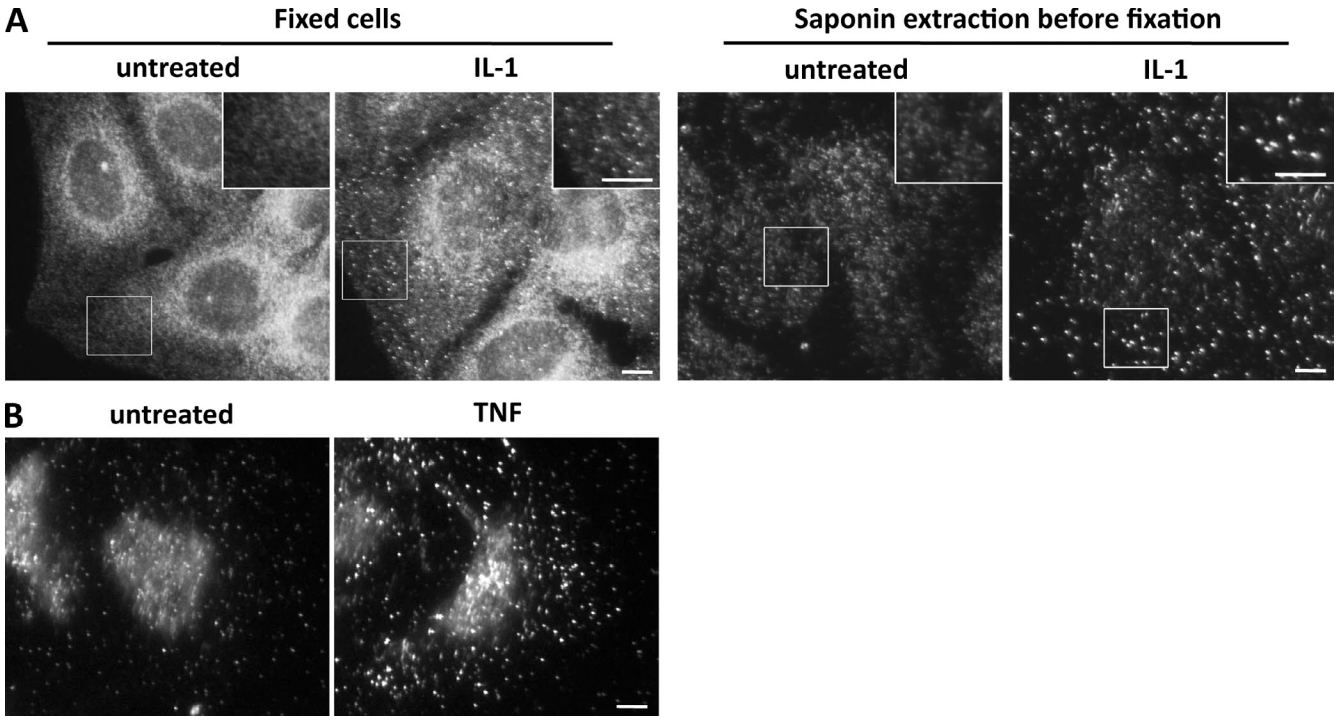


Figure 1. **TNF and IL-1 induce the accumulation of NEMO in punctate structures.** Immunofluorescence analysis of NEMO in U20S cells left untreated or stimulated with IL-1 (A) or TNF (B) for 12 min. In the two right-hand images of A and in B, the cells were subjected to saponin extraction before fixation. The insets in the images show magnified areas (indicated by the boxed regions). Bars, 5 µm.

These results thus show that IL-1– and TNF-induced NEMO-containing structures are enriched in activated IKKs, and they suggest that the local accumulation of NEMO–IKK complexes and the activation of IKK kinases are coordinated events.

NEMO is rapidly and transiently recruited to punctate structures in stimulated living cells

We followed the formation of NEMO-containing structures in living cells by stably reconstituting a NEMO-deficient human fibroblast cell line with GFP-NEMO (Fig. S1 A). NEMO-deficient fibroblasts expressing GFP were used as a control. As expected, the treatment of the control cells with IL-1 did not lead to translocation of the p65/RelA subunit of NF-κB to the nucleus (Fig. S1 B). However, reconstitution with GFP-NEMO restored the NF-κB pathway, as attested by the nuclear translocation of p65 in response to stimulation with IL-1 (Fig. S1 B). IL-1 had no effect on the subcellular distribution of GFP alone, whereas it induced a clear relocalization of GFP-NEMO to small foci (Fig. S1 B) similar to those observed for endogenous NEMO in U2OS cells. We thus used this GFP-NEMO–expressing cell line to visualize, with real-time confocal video microscopy, the formation of NEMO structures in response to treatment with IL-1 or TNF. Unstimulated cells displayed uniform GFP-NEMO staining, which remained constant throughout the time of video acquisition (Video 1). In contrast, the stimulation of GFP-NEMO–expressing cells with IL-1 (Fig. 3 A and Video 2) or TNF (Fig. 3 B and Video 3) induced the rapid and transient recruitment of GFP-NEMO to punctate structures. We then quantified GFP-NEMO–positive foci as a function of time after stimulation (see Materials and methods). IL-1 and TNF induced the formation of GFP-NEMO–containing punctae within a few minutes of stimulation (Fig. 3, A and B). The GFP-NEMO–positive structures appeared more rapidly after stimulation with TNF than after stimulation with IL-1, reaching a maximum at 145 ± 60 s for TNF versus 270 ± 60 s for IL-1. For both cytokines, similar kinetics of disappearance were recorded for GFP-NEMO–containing punctae, which were no longer visible ∼10 min after stimulation in both cases.

Overall, these data show that the exposure of cells to IL-1 and TNF induces the rapid and transient relocalization of NEMO and activated IKK kinases to punctate structures.

NEMO-containing punctae are slow-moving anchored structures located close to the cell surface

An examination of the NEMO-containing punctae induced by IL-1 (Video 2) or TNF (Video 3) suggested that these structures were not highly mobile. We used high-rate total internal reflection fluorescence (TIRF) microscopy to optimize the visualization of these movements. Video tracking was performed for IL-1– and TNF-induced GFP-NEMO–containing punctae (Videos 4 and 5, respectively; see Materials and methods). Representative examples of particle movements are displayed in Fig. S2 A. We found that the GFP-NEMO–containing structures induced by IL-1 or TNF displayed confined random motion. Mean square displacement (MSD) analysis (Qian et al., 1991; see Materials and methods) indicated that these structures were probably anchored (Fig. S2 A). Neither microtubules nor actin fibers seemed to be involved in the formation or mobility of the NEMO-containing structures (at least in the case of IL-1), as no differences in the timing of

Downloaded from on June 15, 2017

Published January 20, 2014

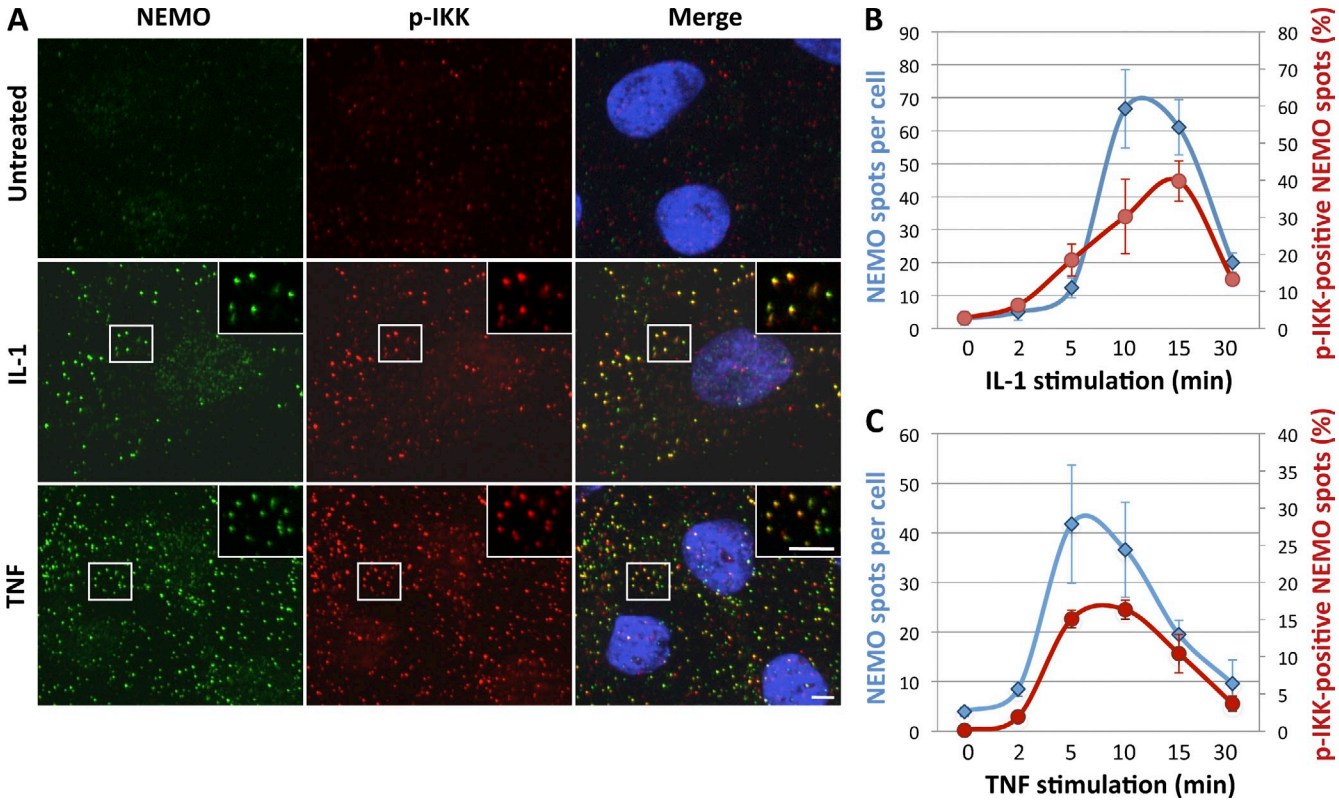


Figure 2. **NEMO and phosphorylated IKKs concentrate into punctate structures in response to cytokine stimulation.** (A) U20S cells left untreated or treated with IL-1 (12 min) or TNF (5 min) were subjected to saponin extraction before fixation and processed for the detection of NEMO (green) and phospho-IKKs (p-IKK, red) by immunofluorescence. Nuclei were stained with DAPI (blue). The insets in the images show magnified areas (indicated by the boxed regions). Bars, 5 µm. (B and C) The number of NEMO foci (blue diamonds) and pIKK-positive NEMO foci (red circles) per cell were quantified after IL-1 (B) and TNF (C) stimulation. Data are presented as mean values ± SD (error bars; $n > 40$ cells analyzed).

their appearance, their movement, or their type of motion were observed between control cells and cells treated with drugs interfering with the polymerization of microtubules (nocodazole) or actin (cytochalasin D and latrunculin B; and Fig. S2 A).

We then investigated the mobility of NEMO in the TNF- and IL-1–induced structures. We explored this issue by performing FRAP experiments in which we first photobleached GFP-NEMO molecules in the TNF- and IL-1–induced structures and then monitored the recovery of the GFP signal over time. These experiments revealed that the recovery of the GFP signal (i.e., the repopulation of the structures with NEMO molecules) was rapid (4.6 ± 3.0 s and 12.1 ± 11.0 s for TNF and IL-1, respectively; Fig. S2 B). It reached a plateau of ∼60% the initial values (corresponding to the mobile fraction of GFP-NEMO), with no further change thereafter, even a long time after photobleaching (Fig. S2 B and Videos 6 and 7). These results suggest the possible existence of two populations of NEMO molecules coexisting in the cytokine-induced structures: an immobile fraction that may constitute the core of the structure (∼40% of the NEMO pool) and a highly diffusible fraction responsible for the rapid turnover of NEMO. The faster signal recovery observed for TNF than for IL-1 may indicate that the rate of turnover of NEMO is higher in TNF- than in IL-1–induced structures.

TIRF experiments indicated that both TNF- and IL-1–induced NEMO-containing structures were present at the cell periphery. We localized cytokine-induced NEMO structures more precisely with respect to the plasma membrane, using GFP-NEMO–expressing cells that were detached from culture dishes and then stimulated with TNF or IL-1 in suspension. This procedure makes it easier to distinguish between the cell periphery and the central cytoplasm than in adherent cells, which are relatively flat. We found that the GFP-NEMO–containing punctae induced by both cytokines were located mostly very close to the plasma membrane (Fig. S3 A). For confirmation that the NEMO-containing structures were indeed localized close to and anchored in the plasma membrane, we isolated lateral and basal membrane patches from TNF- and IL-1–stimulated U2OS cells with a hypotonic shock–based procedure (Drees et al., 2005). TNF- and IL-1–induced NEMO-containing punctae were indeed clearly detected on such membrane preparations (Fig. S3 B), which confirmed that these structures were anchored either directly or indirectly to the plasma membrane.

As our results indicated that TNF and IL-1 induced the recruitment of NEMO to complexes anchored at the plasma membrane, we then investigated whether the NEMO-containing structures colocalized with the activated TNF or IL-1 receptors (TNF-R and IL-1R, respectively). We tested this hypothesis by incubating cells successively at 4°C with biotinylated cytokines and Alexa Fluor 488–tagged avidin, and then transferring them to 37°C to allow activation. We found that the NEMO-containing foci were clearly colocalized with biotinylated TNF-bound receptors (Fig. 4 A), but that they were never colocalized with

Downloaded from on June 15, 2017

Published January 20, 2014

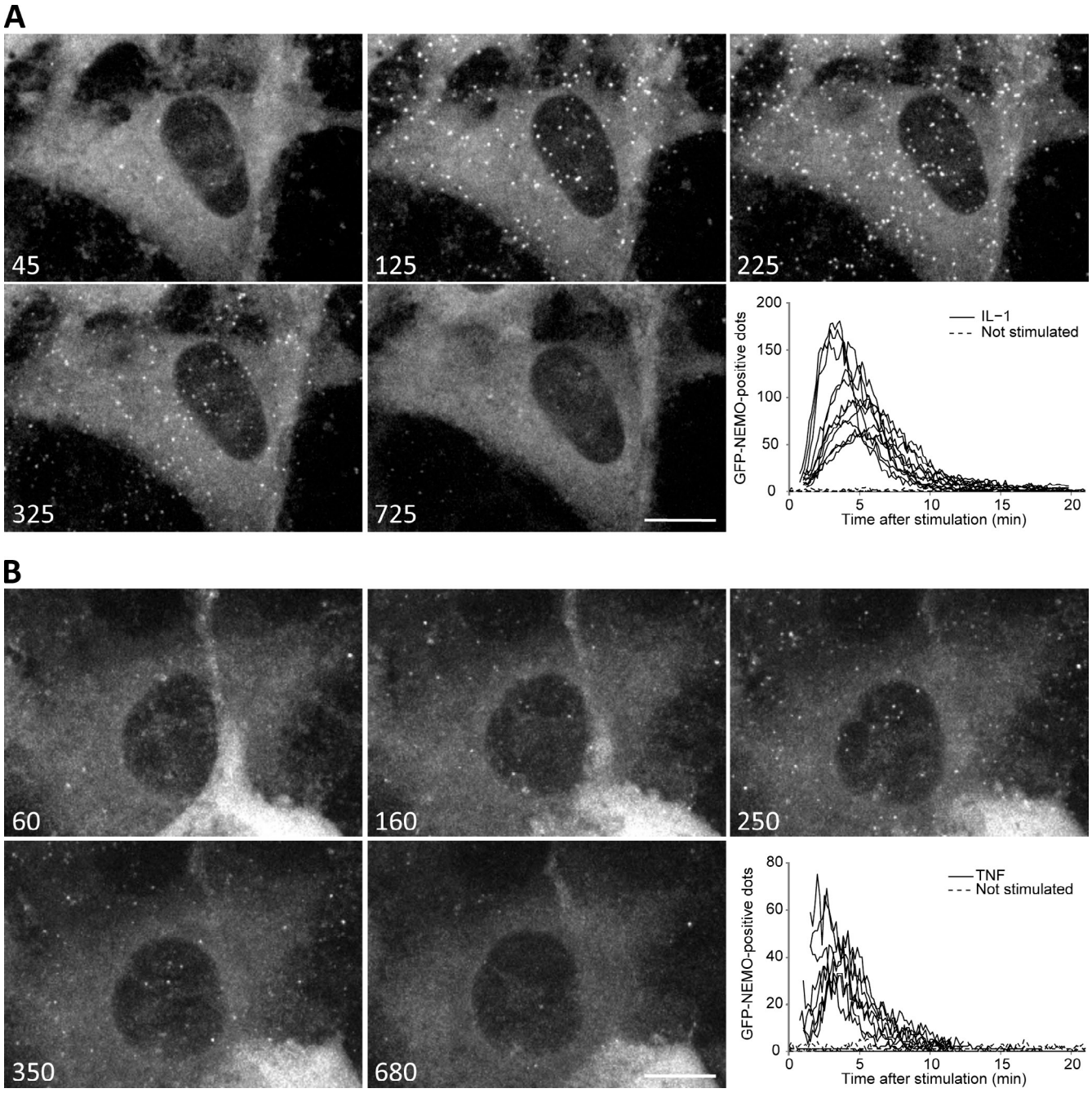


Figure 3. **IL-1– and TNF-induced recruitment of NEMO to punctate structures is a rapid and transient event.** GFP-NEMO–expressing fibroblasts were treated with IL-1 or TNF, and movies were acquired by video microscopy. Still images (at the times indicated, in seconds) after IL-1 (A) and TNF (B) stimulation are presented. These images were extracted from a single representative experiment out of 13 repeats (for IL-1 stimulation) and 9 repeats (for TNF stimulation). The graphs show the number of IL-1– (A) and TNF-induced (B) GFP-NEMO–containing spots per cell (determined as described in the Materials and methods). Each curve represents the number of spots detected in individually recorded cell. Bars, 10 µm.

biotinylated IL-1–bound receptors (Fig. 4 B). As controls, we confirmed that NEMO foci were not observed in noninduced cells (kept at 4°C) and that the signal observed with biotinylated cytokines was abolished by competition with unlabeled ligands (Fig. 4, A and B). Quantitative analysis confirmed that NEMO-containing clusters colocalized with ligand-bound TNF-R after 5 and 15 min of stimulation, but not with ligand-bound IL-1R at either time point (Fig. 4 C).

Together, our observations show that both IL-1 and TNF induce the formation of NEMO-containing clusters at the cell periphery, and that these structures are anchored to the plasma membrane. However, these structures colocalized with the activated TNF-R, but not with the activated IL-1R.

NEMO-containing structures induced by IL-1 also contain IRAK1

Our finding that IL-1–induced NEMO-containing clusters do not colocalize with the IL-1R is consistent with previous reports indicating that the NEMO–IKK complex is activated at some

Downloaded from on June 15, 2017

Published January 20, 2014

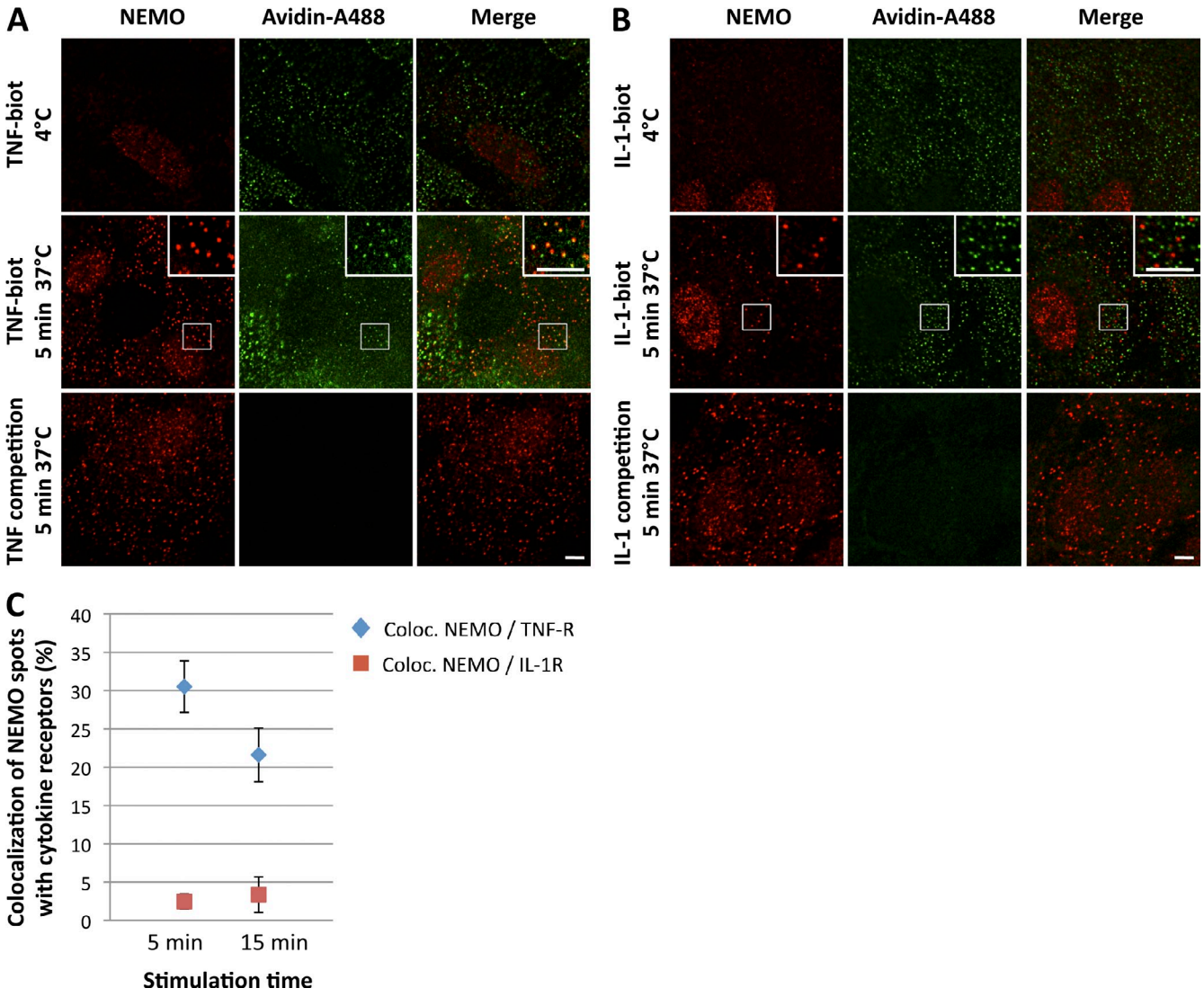


Figure 4. **NEMO-containing structures colocalize with the activated TNF receptor but not with the activated IL-1R.** U2OS cells were incubated successively with biotinylated-TNF (A) or biotinylated-IL-1 (B) and avidin-A488 at 4°C. Cells were fixed directly or shifted to 37°C conditions for 5 min to allow stimulation. NEMO (red) and the activated TNF-R or IL-1R (avidin-A488, green) were detected by immunofluorescence. Competition experiments with unlabeled cytokines (in excess) were performed after the first incubation with biotinylated cytokines to assess probe specificity. The insets in the images show magnified areas (indicated by the boxed regions). Bars, 5 µm. (C) Quantification of the colocalization of NEMO and the activated TNF-R (blue diamonds) and activated IL-1R (red boxes) after 5 and 15 min of stimulation. Data are presented as mean values ± SD (error bars; $n > 100$ cells analyzed).

distance from the activated IL-1-R. Indeed, it has been shown that, upon IL-1 stimulation, IRAK1 dissociates from the IL-1R and recruits the NEMO–IKK complex by interacting with NEMO (for review see Verstrepen et al., 2008). We therefore investigated the possible redistribution of IRAK1 to punctate structures in response to IL-1 stimulation. We found that IRAK1 did indeed form punctate structures in response to stimulation with IL-1 (Fig. 5 A). Most of the IL-1–induced clusters contained both NEMO and IRAK1, but some clusters were positive only for IRAK1. This suggested that the kinetics of formation of IRAK1- and NEMO-containing structures might differ. We investigated this possibility by conducting a quantitative analysis of NEMO and IRAK1 punctae from NEMO/IRAK1 coimmunofluorescence images obtained after a time course of IL-1 stimulation. We found that the kinetics of appearance of NEMO- and IRAK1-containing structures were similar, whereas their kinetics of disappearance differed (Fig. 5 B). Indeed, whereas NEMO-containing structures started to disappear after 15 min of IL-1 stimulation, IRAK1-containing structures remained for longer periods of time. This may reflect an initial phase of association of NEMO with IRAK1 (0–15 min), followed by a phase of NEMO dissociation from IRAK1-containing structures (15–40 min), which are maintained in the cells.

The formation of NEMO-containing clusters requires upstream NF-κB regulators in response to IL-1

The requirement for adaptor proteins is well documented for TNF, for which the complex remains associated with the receptor, but the need for adaptors is much less clear for IL-1, particularly as concerns the kinetics of association and dissociation of the signaling components. We thus determined whether the signaling

Downloaded from on June 15, 2017

Published January 20, 2014

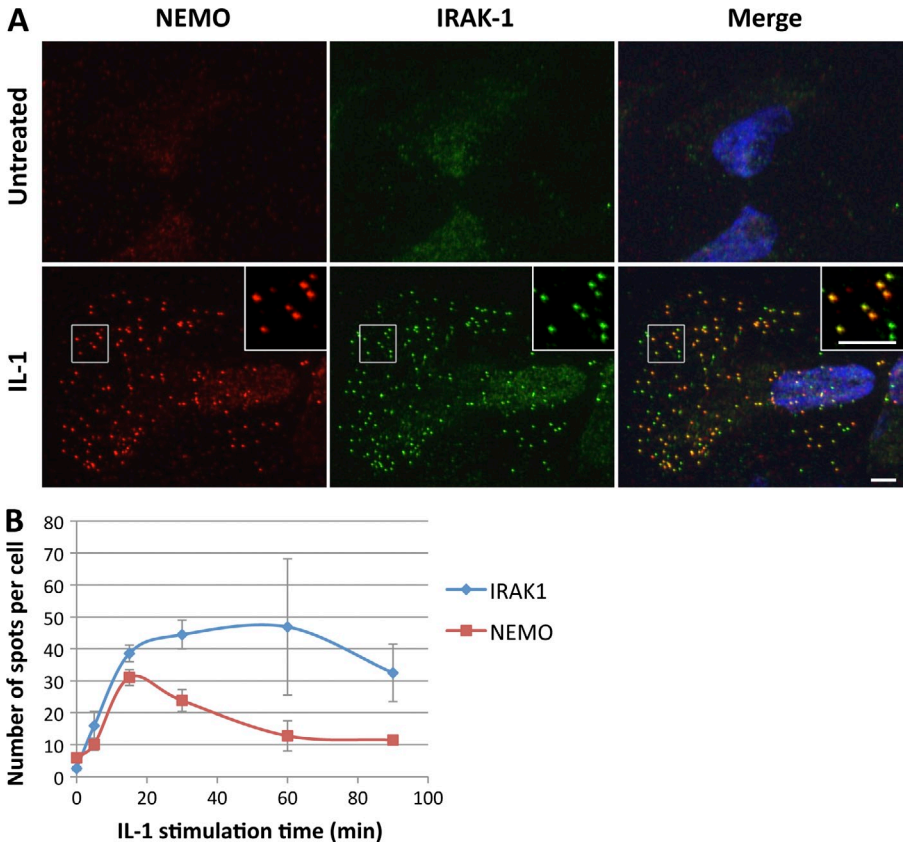


Figure 5. **NEMO and IRAK1 display partial colocalization in punctate structures in response to IL-1.** (A) Immunofluorescence images of NEMO (red) and IRAK1 (green) in U2OS cells left untreated or stimulated with IL-1 for 15 min. Nuclei were stained with DAPI (blue). The insets in the images show magnified areas (indicated by the boxed regions). Bar, 5 µm. (B) Quantification of the number of foci per cell positive for NEMO (red squares) or IRAK1 (blue diamonds) was performed for a time-course of IL-1 stimulation, and the results are presented as mean values ± SD (error bars; $n > 950$ cells analyzed).

components known to be involved in the activation of NF-κB in response to IL-1 were required for the formation of punctate structures containing NEMO and/or IRAK1. We explored this issue using human mutant cell lines (NEMO$^{-/-}$, MyD88$^{-/-}$, and IRAK4$^{-/-}$) isolated from patients or an engineered cell line (IRAK1$^{-/-}$ HEK-293 cells). We treated these cells with IL-1 and checked for the presence of NEMO and IRAK1 punctae with immunofluorescence assays. We monitored NF-κB activation in parallel by assessing the nuclear translocation of p65 (Table 1). In human fibroblasts derived from NEMO-, MyD88-, and IRAK4-deficient patients, and in HEK-293 cells lacking IRAK1, we detected no NEMO-containing punctae after IL-1 stimulation (very few NEMO-containing punctae were observed in the case of IRAK4-deficient fibroblasts). The nuclear translocation of p65 was not observed in any of these IL-1–treated cell lines. Thus, the formation of NEMO-containing punctate structures was associated with NF-κB activation. The formation of IL-1–induced NEMO-containing structures and p65 nuclear translocation was fully restored by complementing IRAK1$^{-/-}$ cells with the IRAK1 cDNA. IL-1–induced IRAK1 structures were not observed in the absence of MyD88, but such structures were clearly detected in the absence of NEMO or IRAK4. Overall, these data indicate that the NF-κB activation signal cannot be transduced just by the formation of IRAK1 punctae; NEMO recruitment is also required.

NEMO and IRAK1 are ubiquitinated in IL-1–induced structures

IL-1 stimulation is known to induce the ubiquitination of IRAK1, which is crucial for the recruitment of NEMO, leading to the activation of NF-κB. The ubiquitination of NEMO in response to IL-1 and TNF has also been reported (Tang et al., 2003; Walsh

Table 1. **Signaling components required for the formation of NEMO- and IRAK1-containing structures and NF-κB activation in response to IL-1**

Cell genotype	Cell type	NEMO-containing clusters	IRAK1-containing clusters	NF-κB activation (nuc. p65)
Control fibro.	Human fibroblast	+++	+++	+++
NEMO$^{-/-}$	Human fibroblast	–	+++	–
MyD88$^{-/-}$	Human fibroblast	–	–	–
IRAK1$^{-/-}$	HEK-293	–	–	–
IRAK1$^{-/-}$ compl. IRAK1	HEK-293	+++	+++	+++
IRAK4$^{-/-}$	Human fibroblast	+/–	+++	+/–

The indicated cell lines were stimulated with IL-1 for 15 min and analyzed by immunofluorescence for the presence of NEMO or IRAK1 foci and for the nuclear translocation of p65. "IRAK1$^{-/-}$ compl. IRAK1" refers to IRAK1$^{-/-}$ cells transiently reconstituted with IRAK1. "+++" indicates that the event was fully observed (same frequency as for IL-1–treated control cells). "+/–" indicates that the event was observed with a frequency <10% that for control cells. "–" indicates that the event was not observed.

Downloaded from on June 15, 2017

Published January 20, 2014

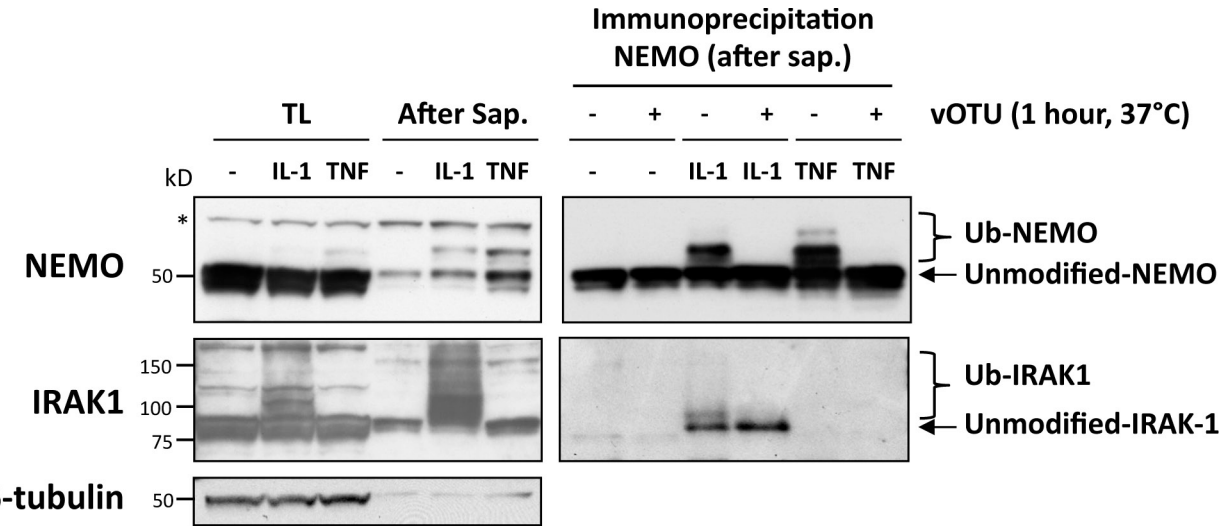


Figure 6. **NEMO and IRAK1 are ubiquitinated in IL-1–induced aggregates.** U2OS cells left untreated or stimulated with IL-1 or TNF (for 12 and 5 min, respectively) were either directly lysed (TL) or permeabilized with saponin before lysis (After Sap.) as described in the Materials and methods. (right) NEMO immunoprecipitates from saponin-extracted cells were left untreated (−) or treated (+) with the vOTU deubiquitinase for 1 h at 37°C. Protein extracts were analyzed by immunoblotting for the detection of NEMO, IRAK1, and β-tubulin, as indicated.

et al., 2008). We therefore investigated whether the ubiquitination of IRAK1 and NEMO occurred in IL-1– or TNF-induced structures. We used our procedure for permeabilizing living cells with saponin (making it possible to extract cytosolic/soluble NEMO and IRAK1 while preserving NEMO- and IRAK1-containing superstructures), followed by protein extraction and immunoblot analysis. The treatment of IL-1–induced cells with saponin led to a strong enrichment in slowly migrating forms of NEMO and IRAK1 (Fig. 6), which were much less visible in the absence of saponin treatment. A similar enrichment in slowly migrating NEMO species was also observed in response to TNF, whereas, as expected, IRAK1 was not modified in response to this cytokine. We investigated whether the apparent modification of NEMO and IRAK1 involved ubiquitination by immunoprecipitating NEMO from saponin-extracted fractions and treating it with the viral ovarian tumor domain (vOTU) deubiquitinase from Crimean Congo hemorrhagic fever virus (Frias-Staheli et al., 2007). The vOTU treatment of NEMO immunoprecipitates led to the disappearance of slowly migrating forms of NEMO (after IL-1 and TNF stimulation) and associated IRAK1 molecules (after IL-1 stimulation; Fig. 6), demonstrating that these proteins were indeed ubiquitinated within the punctate structures.

K63-linked and linear ubiquitination are required for the induction of NEMO-containing structure formation by IL-1 but not by TNF

Many studies have shown that atypical ubiquitin chains, such as K63-linked and linear chains in particular, are involved at different levels of the NF-κB signal transduction pathways. Our observation that both IL-1 and TNF induced the relocalization of NEMO into punctate structures led us to investigate the importance of nondegradative ubiquitin chains, focusing particularly on K63-linked and linear chains.

We investigated the role of K63-linked ubiquitination using an engineered U2OS cell line in which K63-linked ubiquitin chains can be selectively inhibited in an inducible manner (Xu et al., 2009). This inhibition is achieved by the doxycycline (Dox)-induced silencing of endogenous ubiquitin and its concomitant replacement with a mutant ubiquitin molecule (K63R), which is unable to elongate K63-linked chains. Consistent with published results (Xu et al., 2009), we showed that the replacement of endogenous ubiquitin with K63R mutant ubiquitin abolished NF-κB activation by IL-1, but not by TNF, as shown by the phosphorylation of IKK kinases and the degradation of IκBα (Fig. S4). In the control U2OS cell line (shUb-Ub^{WT}) cultured in the presence or absence of Dox, a clear relocalization of NEMO into punctate structures was observed after stimulation with IL-1 (Fig. 7 A). In the Dox-treated shUb-Ub^{K63R} U2OS cell line with impaired K63-linked chain formation, the situation was clearly different, as IL-1 did not induce such a redistribution of NEMO. Quantitative analysis confirmed the absence of NEMO-containing structures in Ub^{K63R}–expressing cells treated with IL-1 (Fig. 7 B). In the case of TNF stimulation, NEMO-containing structures clearly formed in both the shUb-Ub^{WT} and shUb-Ub^{K63R} U2OS cell lines, independently of Dox treatment (Fig. 7 C). Quantitative analysis confirmed that TNF induced similar numbers of NEMO-containing structures in all conditions tested (Fig. 7 D).

Thus, K63-linked ubiquitination is indispensable for the formation of NEMO-containing structures and NF-κB activation in response to IL-1, but is dispensable for both events in response to TNF.

We investigated the importance of linear ubiquitination for the formation of NEMO-containing structures using human fibroblasts isolated from patients lacking HOIL1, one of the three components of the LUBAC complex (Boisson et al., 2012). In control human fibroblasts exposed to IL-1 or TNF, NEMO

Downloaded from on June 15, 2017

Published January 20, 2014

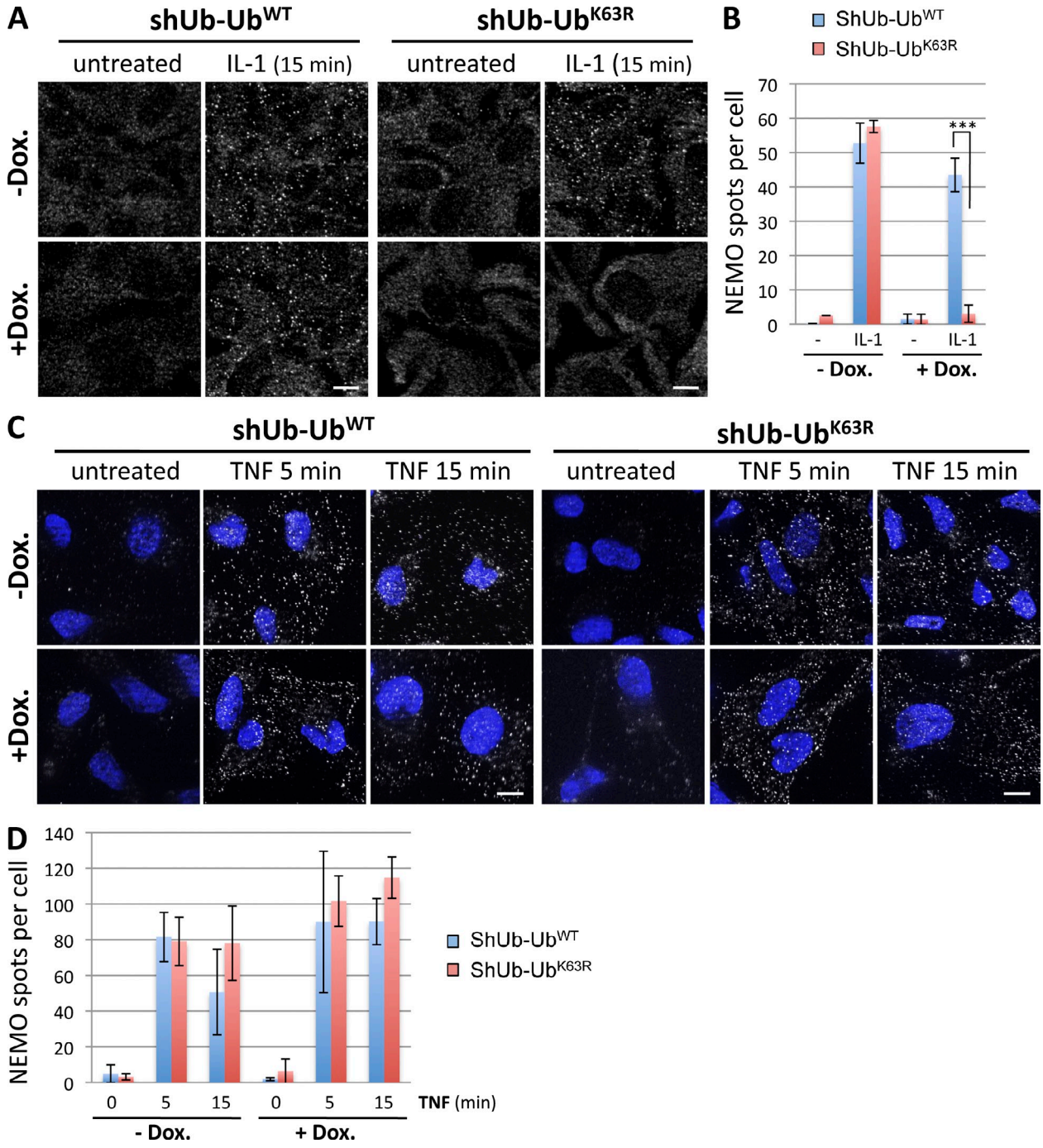


Figure 7. **K63-linked ubiquitination is required for the formation of NEMO-containing structures in response to IL-1, but not TNF.** U2OS-shUb-Ub^{WT} and U2OS-shUb-Ub^{K63R} cells cultured in the absence (−Dox.) or presence (+Dox.) of Dox (1 µg/ml) for 3 d were stimulated with IL-1 (A) or TNF (C), as indicated. Immunofluorescence assays were performed to detect NEMO. In C, cells were permeabilized with saponin before fixation and immunofluorescence assays. Nuclei were stained with DAPI (blue). Bars, 10 µm. (B and D) Numbers of NEMO spots per cell in the experiments presented in A and C, respectively, presented as mean values ± SD (error bars; $n > 50$ cells analyzed). Unpaired t tests were used to assess the significance of differences. ***, $P < 0.001$.

was rapidly redistributed into punctate structures (Fig. 8 A). In HOIL1-deficient fibroblasts, IL-1 failed to induce such a redistribution of NEMO (Fig. 8 A), whereas TNF clearly induced NEMO-containing structures, albeit in smaller numbers than in control cells (mostly after 12 min of TNF stimulation). Quantitative analysis (Fig. 8 B) confirmed these results. Biochemical analysis (Fig. 8 C) reproduced our published data (Boisson et al., 2012) showing that NF-κB activation (assessed by monitoring the phosphorylation of IKK kinases and the degradation of IκBα) is weaker in HOIL1-deficient cells than in control cells, in response to both cytokines. As previously reported, the defect in NF-κB activation observed in HOIL1-deficient cells was more pronounced in response to IL-1 than TNF, as shown by the large decrease in the pIKK signal after IL-1 stimulation (Fig. 8 C), and even more clearly on transcriptome analysis (Boisson et al., 2012).

Downloaded from on June 15, 2017

Published January 20, 2014

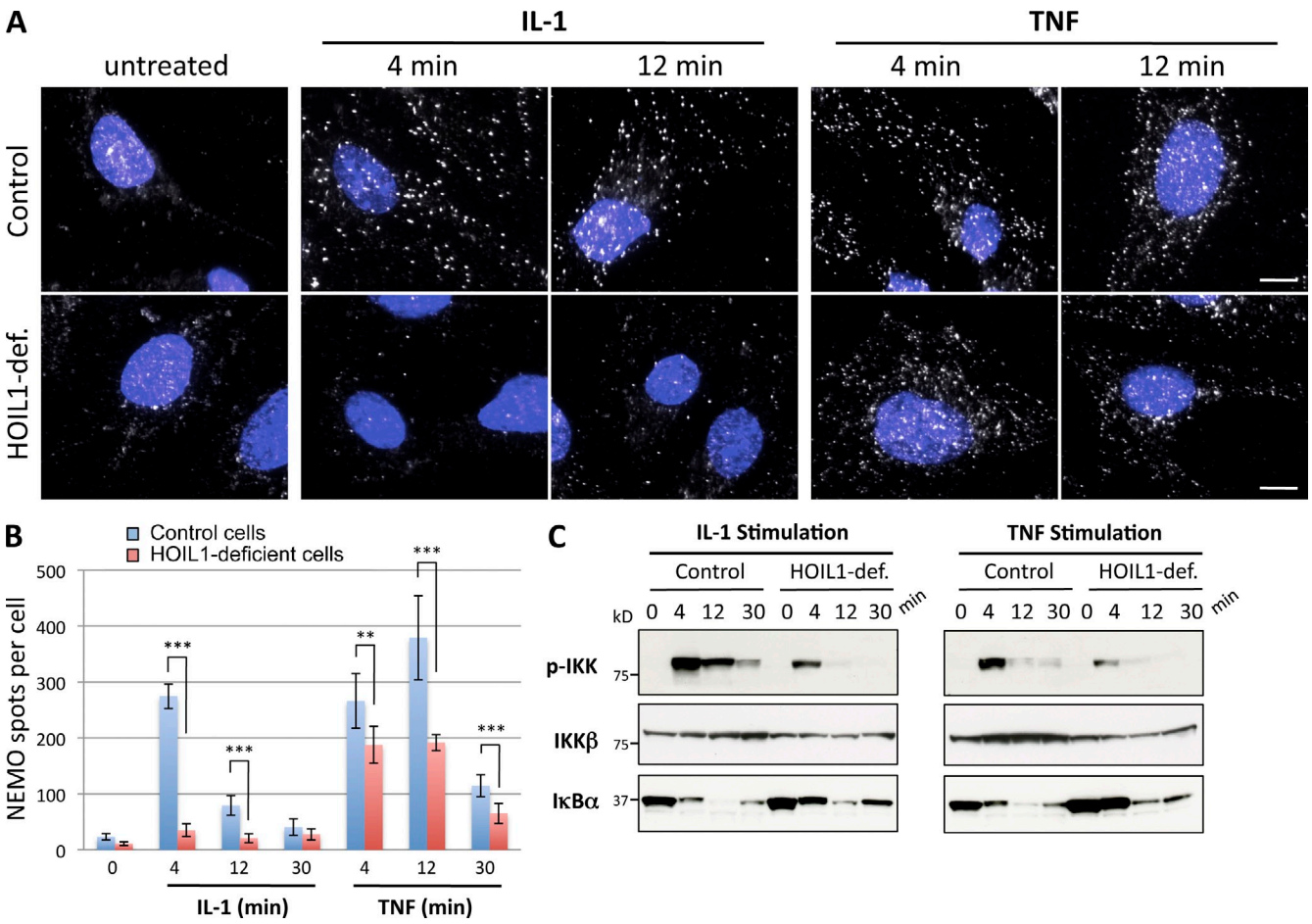


Figure 8. **Linear ubiquitination is required for the formation of NEMO-containing structures in response to IL-1, but not TNF.** (A) Control and HOIL1-deficient human fibroblasts were left untreated or stimulated with TNF or IL-1, as indicated. Cells were permeabilized with saponin before fixation and then processed for the detection of NEMO by immunofluorescence. Nuclei were stained with DAPI (blue). Bars, 10 µm. (B) The number of NEMO spots per cell in the experiment presented in A presented as mean values ± SD (error bars; $n > 60$ cells analyzed). Unpaired *t* tests were used to determine the significance of differences. ***, $P < 0.001$; **, $P < 0.01$. (C) NF-κB activation status in control and HOIL1-deficient cells stimulated with IL-1 and TNF for the times indicated was monitored by the detection of phosphorylated IKKα/β (p-IKK), IKKβ, and IκBα on immunoblots.

Finally, we performed immunofluorescence experiments with a recently engineered anti-linear ubiquitin chain antibody (Matsumoto et al., 2012). We found that stimulation with IL-1 or TNF led to a pronounced accumulation of linear ubiquitin chains, which colocalized with NEMO (Fig. 9).

Together, these results (summarized in Table S1) indicate that K63-linked ubiquitination and linear ubiquitination are required for the formation of NEMO-containing structures and for NF-κB activation in response to IL-1, but that these processes play a minor role in the formation of NEMO-containing structures and in NF-κB activation in response to TNF.

Discussion

In this study, we found that the induction of NF-κB signaling by two proinflammatory cytokines—TNF and IL-1—led to the rapid, juxtamembrane accumulation of NEMO in punctate structures. The phosphorylated and, therefore, activated forms of the IKK kinases were also concentrated in these NEMO-containing structures, which suggests that they may constitute a local platform essential for the initiation of downstream NF-κB signal transduction. We investigated the role of K63-linked and linear ubiquitin chains in response to TNF and IL-1. Using cells lacking either K63-linked chains or LUBAC-mediated linear ubiquitination, we were able to show a clear difference in the contribution of these two types of nondegradative ubiquitination to the TNF and IL-1 responses. Indeed, whereas the IL-1–mediated clustering of NEMO clearly required both K63-linked and linear ubiquitination, these two types of ubiquitination appeared to be dispensable in the response to TNF.

By various imaging techniques, we showed that the exposure of cells to TNF, IL-1, and lipopolysaccharides (LPS; not depicted) led to the local recruitment of NEMO to small punctate particles. The size of both the TNF- and IL-1–induced NEMO-containing structures was estimated at 250 ± 150 nm (estimated from the measured sizes of GFP-NEMO–positive clusters in Fig. 3). These structures formed within a few minutes of cytokine exposure. This phenomenon was transient, because the NEMO-containing structures had almost totally disappeared after 15–45 min (depending on the stimulus and the cell type) even in the continuous presence of the cytokine. The kinetics of this event suggested a role in the initiation of NF-κB signaling and,

Downloaded from on June 15, 2017

Published January 20, 2014

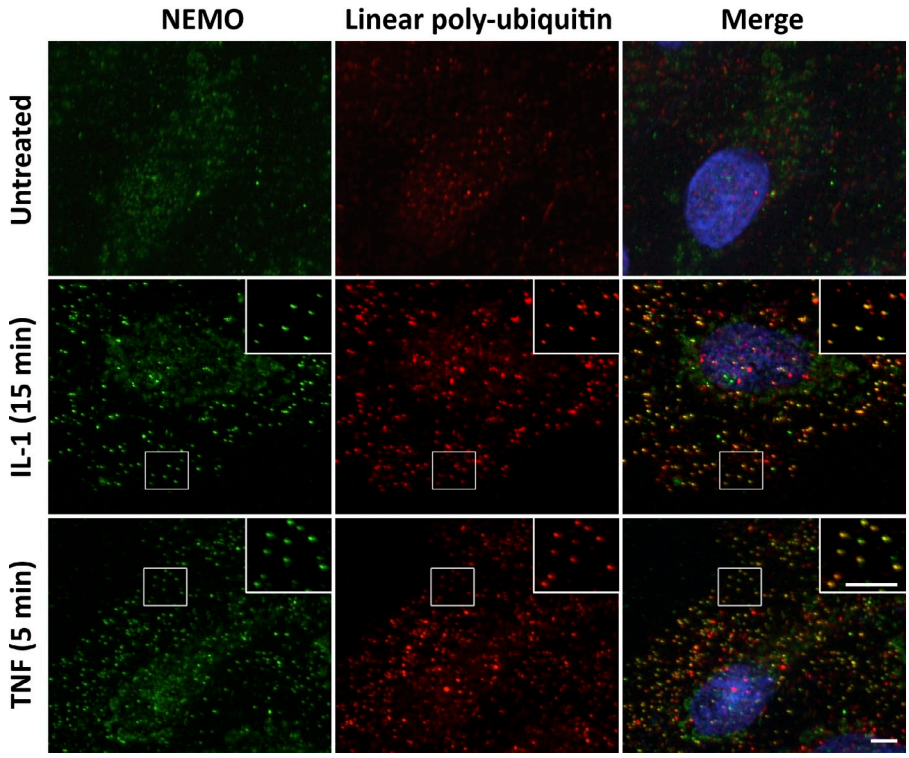


Figure 9. **Linear ubiquitin chains are enriched in NEMO-containing foci in response to IL-1 and TNF.** U2OS cells were left untreated or stimulated with IL-1 or TNF, as indicated. Cells were permeabilized with saponin before fixation and processed for the detection of NEMO (green) and linear ubiquitin chains (red) by immunofluorescence. Nuclei were stained with DAPI (blue). The insets in the images show magnified areas (indicated by the boxed regions). Bar, 5 µm.

possibly, its down-regulation. Indeed, a role for this NEMO clustering event as a prerequisite for the activation of NF-κB is supported by the following observations: (1) this event was very rapid and always preceded IκB's degradation and the nuclear translocation of p65/RelA (unpublished data); (2) aggregates of NEMO also contained phosphorylated/activated IKK kinases, with NEMO aggregation and IKK activation occurring simultaneously; and (3) NEMO clustering was never observed in situations in which NF-κB signaling was impaired (see Table 1), such as in IRAK1-deficient cell lines and patient-derived cells lacking signaling adaptor molecules, such as MyD88 or IRAK4.

What triggers the local accumulation of NEMO and why is it important for downstream signaling events? It has been suggested that NEMO is recruited to adaptor molecules in response to TNF and IL-1 stimulation: RIP1 and IRAK1, respectively. We can therefore speculate that higher-order assemblies containing these adaptor intermediates might form within cells in response to cytokine stimulation. Indeed, IRAK1 formed punctae that colocalized with NEMO in response to IL-1. Interestingly, it has recently been suggested that higher-order assemblies may constitute a common mechanism in immune signaling (Wu, 2013). Unlike G protein–coupled receptors (GPCRs) and receptor tyrosine kinases (RTK), TNF-R and IL-1R have no enzymatic activity and are not directly coupled to intracellular enzymes. In the case of these two receptors, higher-order assemblies might provide a signal amplification process, together with the temporal and spatial control of signal transduction (Wu, 2013). The signal-dependent, controlled, nucleated formation of large assemblies has recently been demonstrated for the CARMA1/Bcl10/MALT1 signalosome, which mediates antigen receptor-induced NF-κB signaling (Qiao et al., 2013). The local accumulation of NEMO in association with IKK kinases might also be directly involved in the activation of these kinases through a proximity-induced transphosphorylation mechanism, as previously suggested (Ghosh and Karin, 2002). The fact that a forced subcellular concentration of NEMO is sufficient to activate the IKKs and to transmit NF-κB signaling is consistent with this hypothesis (Weil et al., 2003).

The formation of cytokine-induced NEMO-containing structures was a transient event. Their disappearance may correspond to one of the many negative feedback mechanisms responsible for ensuring the transient nature of the NF-κB response (Ruland, 2011). The NEMO-containing structures were enriched in ubiquitin (linear polyubiquitin at least), which may act as a scaffold, stabilizing the various components of the structures described here (many of which, including NEMO, contain ubiquitin-binding domains). We can speculate that the activity of deubiquitinases, such as CYLD, A20, and OTULIN, might dissociate these higher-order complexes, thereby curtailing the signal.

Stimulation with either TNF or IL-1 induced the formation of NEMO-containing structures anchored at the plasma membrane. However, we observed a clear difference in the localization of these NEMO-containing structures relative to the activated cytokine receptors. Indeed, whereas NEMO-containing structures appeared to be part of the TNF-RSC, they were clearly separate from the activated IL-1R. This difference is consistent with published data showing that, in response to TNF, the NEMO–IKK complex is recruited to the TNF-RSC via the TNF-associated RIP1 protein (Zhang et al., 2000; Wu et al., 2006; Haas et al., 2009), whereas, in response to IL-1, the NEMO–IKK complex associates with IRAK1 once it has detached from the activated IL-1R (Conze et al., 2008; Ordureau et al., 2008; Windheim et al., 2008). Other groups have suggested that IKK complex activation takes place in the cytosol,

Downloaded from on June 15, 2017

Published January 20, 2014

independent of IRAK1 but dependent on a complex containing TRAF6-TAK1-TAB1-TAB2 (Jiang et al., 2002). IL-1 stimulation resulted in the formation of a complex anchored at the plasma membrane, containing both NEMO and IRAK1, but also activated IKK kinases. Our conclusion that IL-1 stimulation induces the relocalization and activation of the NEMO–IKK complex at the plasma membrane and not in the cytosol is supported by: first, our confocal imaging data for IL-1–stimulated adherent and detached cells showing that NEMO- and IRAK1-positive structures are localized at the cell periphery; second, the visualization of IL-1–induced NEMO-containing structures by TIRF microscopy, allowing a detection no more than 100 nm below the plasma membrane; and third, by the fact that we could observe NEMO-containing structures on isolated lateral and basal membrane patches. Our study therefore indicates that after stimulation with IL-1, the NEMO–IKK complex is stably associated with the plasma membrane either directly or indirectly, possibly through an unidentified membrane-bound adaptor molecule.

The NEMO-containing structures induced by TNF and IL-1 had different subcellular distributions, but our video microscopy analyses revealed a similar mobility of these structures in response to TNF and IL-1. In both situations, NEMO-containing structures were not highly mobile and were not associated with the actin or microtubule networks. The displacements measured indicate that the structures containing NEMO were anchored, but FRAP experiments showed that a large proportion of NEMO molecules were highly mobile, moving in and out of these structures. Based on the apparent rapid cycling of NEMO in these structures, we suggest that they may constitute local organizing centers for the recruitment and activation of NEMO–IKK complexes. Once activated, NEMO–IKK complexes may leave these organizing centers, allowing the rapid entry of new complexes in a cyclic manner. The activated IKK complexes may then phosphorylate their targets, the most important of which is the IκBs, in the cytosol. This hypothesis is supported by pioneering work from D. Wallach (Zhang et al., 2000) showing that activation of the IKK complex by TNF occurs at the plasma membrane, whereas IKK complexes competent for IκB phosphorylation are located in the cytosol. Our detection of phosphorylated IκBα in the cytosol, but never in TNF- and IL-1–induced NEMO-containing structures (unpublished data), suggests that NEMO–IKK complexes may first be activated in the membrane-associated structures described here, before their translocation to the cytoplasm, where the IKK kinases may finally reach their targets.

Non-degradative ubiquitination, particularly of the K63-linked and linear types, has emerged as a key mediator of NF-κB signaling. These two types of ubiquitin modification have been reported to occur in response to both TNF and IL-1. However, published data suggest that the relative importance of these two types of modification differs between the responses to these two cytokines (Xu et al., 2009; Boisson et al., 2012). In this study, we show clearly that the local recruitment of NEMO into foci requires both K63-linked and linear ubiquitination in response to IL-1, whereas each of these two types of ubiquitin modification appears to be dispensable in response to TNF. This requirement was fully linked to the activation of NF-κB (see Table S1). K63-linked ubiquitination clearly occurs in response to both TNF and IL-1 (for review see Chen, 2012). We show here that linear ubiquitin chains accumulate in NEMO-containing structures in response to both stimuli (Fig. 9). One possible interpretation is that K63-linked and linear ubiquitination may have specific, nonredundant roles in the signal transmission induced by IL-1, whereas these two types of modification may have overlapping functions in response to TNF. It is also possible that other types of ubiquitin chains, such as K11-linked chains (Dynek et al., 2010), may play a compensatory role in the TNF response. It has recently been shown that mixed ubiquitin chains composed of both K63-linked and linear chains are generated in response to IL-1, and that the presence of K63-linked chains is a prerequisite for LUBAC-mediated linear ubiquitination (Emmerich et al., 2013). This may explain why these two types of ubiquitin modification appear to be critical for the IL-1 response.

Our results demonstrate that the NF-κB–inducing proinflammatory cytokines TNF and IL-1 induce the rapid and transient formation of macromolecular complexes containing NEMO, and that this is a critical event for the transmission of NF-κB signals. We identified major differences in the distribution, ubiquitin requirement, and dynamics of these structures in response to these two stimuli, reflecting specific features of the pathways involved. The local accumulation of NEMO reported here may be linked to the proposed proximity-induced conformation model, leading to IKK kinase activation. We can speculate that local accumulation of the NEMO–IKK complex is common to other NF-κB activation processes. Interference with or promotion of the formation of these higher-order structures might be relevant in pathological situations in which NF-κB activity is deregulated, such as cancers or immunodeficiencies. Furthermore, the visualization of NEMO–IKK clusters described here constitutes a new NF-κB activation "readout" that could be used for future diagnostic or screening purposes.

Materials and methods

Cell lines, cell culture, and reagents

U2OS and HeLa cells were purchased from ATCC. U2OS-shUb-Ub^{WT} and U2OS-shUb-Ub^{K63R} cells (Xu et al., 2009) were provided by J. Chen (University of Texas Southwestern Medical Center, Dallas, TX). These genetically modified U2OS cell lines were engineered to inducibly express wild-type or K63R mutated ubiquitin in replacement of endogenous ubiquitin using a tetracycline-inducible system. The NEMO-deficient human embryonic fibroblast cell line (Smahi et al., 2000) was provided by A. Smahi (Fondation Imagine, Paris, France). These cells were isolated from a spontaneously aborted female fetus, carrying a homozygous deletion of exons 4–10 of the *nemo* gene, and subsequently immortalized using SV40 large T antigen. NEMO-deficient human fibroblast cell lines stably expressing GFP and GFP-NEMO were generated by transfecting the aforementioned NEMO$^{-/-}$ cells with GFP- or GFP-NEMO–expressing plasmids (described later) and selected on the G418 antibiotic. We isolated several clones from the pool of cells expressing GFP-NEMO by limited dilution. HEK-293 cells lacking IRAK1 (IRAK1$^{-/-}$ or the I1A cell line) were obtained from G. Stark's laboratory (The Lerner Research Institute, Cleveland, OH; Li et al., 1999). These cells were obtained by chemical mutagenesis of human embryonic kidney 293 cells containing an IL-1–regulated herpes thymidine kinase gene, followed by selection with IL-1 and ganciclovir. SV40 large T antigen–immortalized human fibroblasts were derived from healthy individuals; those from HOIL1-, IRAK4-, and MyD88-deficient patients were provided by J.-L. Casanova (Howard Hughes Medical Institute, The Rockefeller University, New York, NY) and C. Picard (Hôpital Necker, Paris, France). HOIL1-deficient fibroblasts were obtained from three patients carrying biallelic

Downloaded from on June 15, 2017

Published January 20, 2014

loss-of-expression and loss-of-function mutations in HOIL1 (Boisson et al., 2012). IRAK4- and MyD88-deficient fibroblasts were obtained from patients carrying homozygous mutations in the *IRAK4* gene (p.E92fsX118/p.E92fsX118; Picard et al., 2011) and *Myd88* (p.E52del/p.E52del; von Bernuth et al., 2008), respectively. HEK-293 cells stably expressing TLR4 were purchased from Invitrogen. All cell lines were cultured in DMEM (Invitrogen) supplemented with 10% FBS, 50 U/ml penicillin, and 50 µg/ml streptomycin. Cells were stimulated with the following cytokines: TNF, biotinylated-TNF, biotinylated-IL-1, and IL-1 (R&D Systems). LPS, cytochalasin D, nocodazole, latrunculin B, and Dox were purchased from Sigma-Aldrich.

Plasmids and antibodies

The GFP-NEMO plasmid was generated by inserting the EGFP cDNA in frame with the 5′ end of the mouse NEMO ORF into the previously described CMV-HA-NEMO vector (Yamaoka et al., 1998). The EGFP plasmid was obtained from Takara Bio Inc. The antibodies used for immunofluorescence detection and for immunoblots were anti-NEMO (rabbit sc-8330 [Santa Cruz Biotechnology, Inc.] and mouse mAb No. 611306 [BD]), rabbit anti–phospho-IKKα/β mAb (ser176/180; 16A6; Cell Signaling Technology), mouse anti-IKKβ mAb (AM8109a; Abgent), rabbit anti–IL-1R1 mAb (04-465; EMD Millipore), mouse anti-IκBα mAb (No. 610690; BD), anti-IRAK1 (rabbit sc-7883 and mouse mAb sc-5288; Santa Cruz Biotechnology, Inc.), rabbit anti-p65/RelA (raised against the peptide sequence ADMDFSALLSQISS; provided by N. Rice, National Cancer Institute Frederick Cancer Research and Development Center, Frederick, MD), mouse anti-HA mAb (HA11 clone 16B12; Eurogentec), mouse anti-actin mAb (A4700; Sigma-Aldrich), and mouse anti–β-tubulin mAb (T4026; Sigma-Aldrich). The mouse monoclonal antibody specific for linear polyubiquitin chains (1F11/3F5/Y102L) was provided by Genentech. The specificity of this antibody resides in its ability to recognize multiple surrounding surface residues present on two ubiquitin molecules connected in a specific orientation as the result of the linear linkage (Matsumoto et al., 2012). Species-specific secondary antibodies coupled to either specific fluorochromes or HRP were obtained from Life Technologies and Vector Laboratories, respectively.

The specificity of the anti-NEMO, anti-IRAK1, and anti-linear ubiquitin chain antibodies used in immunofluorescence is supported by the detection of the same signal using two different anti-NEMO and anti-IRAK1 antibodies (Fig. S5, A and B), and by the absence of detection in NEMO$^{-/-}$, IRAK1$^{-/-}$, and HOIL1-deficient cell lines, respectively (Fig. S5, C–E). For phospho-IKKs, the dot-like staining pattern (colocalizing with NEMO) was observed only in cytokine-treated cells, with a well-referenced monoclonal antibody (16A6; Cell Signaling Technology) that has been successfully used in immunohistochemistry (data provided by the manufacturer).

Cell stimulation and treatments

Cells were stimulated by adding the cytokines directly to the culture medium for the times indicated. Unless specified, cytokines were used at a final concentration of 10 ng/ml. LPS was used at a concentration of 1 µg/ml. The cytoskeleton-interfering drugs cytochalasin D, nocodazole, and latrunculin B were used at concentrations of 20 µM, 10 µg/ml, and 50 µM, respectively. Cells were incubated for 30 min with these drugs before stimulation with cytokines. Dox was used at a concentration of 1 µg/ml. In some cases the cells were permeabilized with saponin before fixation (for immunofluorescence analysis) or lysis (for subsequent biochemical analysis). For this purpose, cells were first washed twice with ice-cold PBS and then treated twice with ice-cold saponin extraction buffer (80 mM Pipes, pH 6.8, 1 mM $MgCl_2$, 1 mM EGTA, and 0.1% saponin) for 2 min and 4 min on ice. They were then washed twice with PBS before fixation or lysis, as described. For the isolation of basal and lateral membrane patches, a modified version of a previously described protocol was used (Drees et al., 2005). All steps were performed on ice, with ice-cold buffers. Cells cultured on coverslips were first washed three times with hypotonic buffer (10 mM Hepes, 10 mM KCl, and 1.5 mM $MgCl_2$) and then incubated for 12 min in hypotonic buffer containing a protease inhibitor cocktail (Complete; Roche). The cells were then disrupted mechanically by pipetting up and down (eight times) directly into the buffer. Cell disruption was verified by microscopy. The coverslips were then rinsed twice with Reiner buffer (10 mM Hepes, 154 mM NaCl, and 7.2 mM KCl) before fixation. Actin immunodetection was performed to locate cell remnants on membrane preparations. We used the following strategy for the detection of activated TNF-R and IL-1R by immunofluorescence: cells cultured on coverslips were incubated for 1 h with 300 ng/ml biotinylated cytokines (R&D Systems) and then for 30 min with 2 µg/ml Alexa Fluor 488–tagged avidin (Life Technologies) at 4°C. The coverslips were then shifted to a temperature of 37°C for 5 or 15 min to allow receptor activation. Noninduced cells (maintained at 4°C) and temperature-shifted cells were then fixed and processed for the detection of NEMO by immunofluorescence. We checked the specificity of the signal obtained for biotinylated cytokines by carrying out competition experiments with excess unlabeled cytokine (2 µg/ml TNF or 1 µg/ml IL-1) for 1 h.

Immunofluorescence, image acquisition, and live-cell imaging

For immunofluorescence, cells cultured on glass coverslips were fixed with either 4% PFA or 100% methanol. After fixation in methanol, cells were progressively rehydrated by successive washes with 85%, 70%, and 50% ethanol in water and two final washes with PBS. PFA-fixed cells were permeabilized with 0.2% Triton X-100. After blocking by incubation with 1% BSA in PBS, the slides were incubated with the primary antibodies, washed, and incubated with species-specific fluorochrome-tagged secondary antibodies. They were washed again and incubated with DAPI (Sigma-Aldrich) to stain the nuclei. The coverslips were mounted in Mowiol supplemented with an anti-fading agent (AF100; Biovalley). Specimens were examined with either an ApoTome imaging system (Imager Z1) equipped with a 63×/1.4 NA oil differential interference contrast (DIC) objective lens or a confocal microscope (LSM700) equipped with a 63× Plan Apochromat/1.4 NA oil objective lens (all from Carl Zeiss). Images were acquired and analyzed with AxioVision or Zen software (Carl Zeiss). For live-cell imaging, cells were cultured in 35-mm-diameter glass-bottomed dishes (MatTek Corporation). Before analysis, Hepes was added to a final concentration of 10 mM. Video microscopy was performed with two spinning-disk confocal microscopes (UltraView VOX and UltraView ERS; PerkinElmer) equipped with a FRAP system (PhotoKinesis). TIRF imaging was done with a CellM system (Olympus) with a Plan Apochromat 100×/1.45 NA objective lens (Olympus). For TIRF experiments, the laser beam was adjusted so that only a thin sheet below the coverslip (~100 nm) was illuminated. Noninvasive imaging required low laser power compensated by a relatively long exposure time. We achieved a frame rate of 2 images/s. FRAP experiments were performed as follows: a single, optically sectioned plane of the cell was imaged every second for 5 frames, and an area of ~3–5 µm in size within the cell was then bleached with a laser beam. Fluorescence recovery was then followed, at a frame rate of 1 image/s. Half recovery times and immobile fractions were derived by fitting a double-exponential model, the simplest model that reliably fitted recovery curves.

Quantification and statistical analysis of immunofluorescence and live-cell imaging data

We used randomly selected fields acquired with a 63× objective lens to determine the number of NEMO-positive foci. Imaris was used for spot detection. For the quantification of NEMO and IRAK1 foci (presented in Fig. 5), we developed image-processing algorithms in ImageJ to remove background noise, to calibrate the detection filters, to segment the foci and nuclei, and to report the total number of foci and cell counts. The program was validated by comparing visual results with program results; error rates were estimated to be <5%.

Colocalization was assessed on randomly selected fields from images, with Fiji (Schindelin et al., 2012) or Imaris (Bitplane AG). The colocalization of NEMO- and p-IKK-positive foci (presented in Fig. 2, B and C) is reported as the percentage of NEMO channel pixels displaying colocalization above the threshold. The colocalization of NEMO and activated cytokine receptors (presented in Fig. 4 C) is reported using thresholded Manders coefficients (Manders et al., 1993; Costes et al., 2004).

Single-focus movements were tracked with the TrackMate plugin of the Fiji image-processing package. Trajectories were then exported and analyzed with MATLAB. The package specifically developed for MSD analysis is publicly available from http://www.mathworks.com/matlabcentral/fileexchange/40692-mean-square-displacement-analysis-of-particles-trajectories. In detail: the MSD function was calculated for each individual trajectory, and its log-log representation was fitted with a linear function, such that if the MSD curve could be modelled by $\rho(r) = \langle r^2 \rangle = \Gamma t^{\alpha}$, then $\log(\langle r^2 \rangle) = f(\log(t))$ was fitted with $\Gamma + \alpha \log(t)$. We fitted individual MSD curves and discarded those for which the R^2 coefficient, reflecting the quality of the fit, was <0.8. These fits supplied us directly with the α values indicated in Fig. S3. According to the modelling study by Qian et al. (1991), an α value of 1 indicates free diffusive movement, a value of α close to 2 indicates movement by active transport, and a value of α <1 indicates a motion constrained in space.

Cell lysis and immunoblotting

Cells were lysed in a buffer containing 50 mM Tris, pH 7.5, 150 mM NaCl, 1% Triton X-100, 1 mM EDTA, and a mixture of protease inhibitors (Complete; Roche) and phosphatase inhibitors (Sigma-Aldrich). Clarified

Downloaded from on June 15, 2017

Published January 20, 2014

lysates were mixed with 4× Laemmli buffer containing DTT and the samples were boiled for 10 min. Proteins were separated by SDS-PAGE and transferred to PVDF membranes (Immobilon; EMD Millipore). Immunoreactive proteins were visualized by chemiluminescence.

Immunoprecipitation of NEMO and in vitro deubiquitination

NEMO was immunoprecipitated from saponin-extracted cells, and lysed in lysis buffer containing protease and phosphatase inhibitors. We added 10 µg of anti-NEMO antibody coupled to agarose beads (sc-8330 AC; Santa Cruz Biotechnology, Inc.) to 700 µg of protein extract and incubated the mixture for 4 h at 4°C. The beads were washed twice in lysis buffer, once in deubiquitination buffer (150 mM Tris, pH 7.5, 50 mM NaCl, and 1 mM DTT), and then were split into two equal batches. One of these batches was treated with 30 µM vOTU and the other was left untreated. Both samples were incubated for 1 h at 37°C, and the reaction was stopped by adding Laemmli buffer containing DTT. The recombinant vOTU deubiquitinase (OTU domain from Crimean Congo hemorrhagic fever virus L1 protein; Frias-Staheli et al., 2007) was produced as a GST fusion protein. The bacterial expression vector encoding GST-vOTU CCHFV-L (1–169) was a gift from A. Garcia-Sastre (Mount Sinai School of Medicine, New York, NY).

Online supplemental material

Fig. S1 shows the GFP-NEMO expression levels, the NF-κB activation levels, and the formation of GFP-NEMO–containing clusters in the human NEMO$^{-/-}$ fibroblast cell line complemented with GFP-NEMO after IL-1 stimulation. Fig. S2 presents the cytokine-induced mobility of the GFP-NEMO–containing structures in the presence of drugs that interfere with actin or microtubules fibers. This figure also presents the molecular dynamics of NEMO in these structures as assessed by FRAP experiments. Fig. S3, related to Fig. 4, shows the localization of TNF- and IL-1–induced NEMO-containing structures relative to the plasma membrane. Fig. S4, related to Fig. 7, shows the IL-1– and TNF-induced NF-κB activation levels in cells deficient for K63-linked chain compared with control cells. Fig. S5 presents the control data demonstrating the specificity of the anti-NEMO, anti-IRAK1, and anti-linear poly-ubiquitin antibodies used in immunofluorescence throughout this study. Videos 1, 2 and 3, related to Fig. 3, show the detection of GFP-NEMO in nonstimulated, IL-1–treated, and TNF-treated cells, respectively. Videos 4 and 5 present the tracked movements of GFP-NEMO–containing structures after TNF and IL-1 stimulation, respectively. Videos 6 and 7 show the repopulation of GFP-NEMO-containing structures after photobleaching in IL-1– and TNF- treated cells, respectively. Table S1 summarizes the data on cytokine-induced NF-κB activation levels and NEMO and IRAK1 foci formation in cells deficient in K63 ubiquitin chains or LUBAC-mediated linear ubiquitination. Online supplemental material is available at http://www.jcb.org/cgi/content/full/jcb.201307172/DC1.

We would particularly like to thank Robert Weil and Pierre Genin for helpful discussions and advice during the course of this work. We thank Jean-Laurent Casanova, Capucine Picard, James Chen, Asma Smahi, and George Stark for providing the cell lines used in this study. We thank Adolfo Garcia-Sastre for the expression vector encoding the viral OTU enzyme.

This work was supported by grants from the "Fondation ARC pour la Recherche sur le Cancer" (No. SFI20121205641) and the "Ligue Contre le Cancer" to E. Laplantine.

Submitted: 26 July 2013
Accepted: 9 December 2013

References

Boisson, B., E. Laplantine, C. Prando, S. Giliani, E. Israelsson, Z. Xu, A. Abhyankar, L. Israël, G. Trevejo-Nunez, D. Bogunovic, et al. 2012. Immunodeficiency, autoinflammation and amylopectinosis in humans with inherited HOIL-1 and LUBAC deficiency. *Nat. Immunol.* 13:1178–1186. http://dx.doi.org/10.1038/ni.2457

Chen, Z.J. 2012. Ubiquitination in signaling to and activation of IKK. *Immunol. Rev.* 246:95–106. http://dx.doi.org/10.1111/j.1600-065X.2012.01108.x

Conze, D.B., C.J. Wu, J.A. Thomas, A. Landstrom, and J.D. Ashwell. 2008. Lys63-linked polyubiquitination of IRAK-1 is required for interleukin-1 receptor- and toll-like receptor-mediated NF-kappaB activation. *Mol. Cell. Biol.* 28:3538–3547. http://dx.doi.org/10.1128/MCB.02098-07

Costes, S.V., D. Daelemans, E.H. Cho, Z. Dobbin, G. Pavlakis, and S. Lockett. 2004. Automatic and quantitative measurement of protein-protein colocalization in live cells. *Biophys. J.* 86:3993–4003. http://dx.doi.org/10.1529/biophysj.103.038422

Courtois, G., and A. Israël. 2011. IKK regulation and human genetics. *Curr. Top. Microbiol. Immunol.* 349:73–95.

Deng, L., C. Wang, E. Spencer, L. Yang, A. Braun, J. You, C. Slaughter, C. Pickart, and Z.J. Chen. 2000. Activation of the IkappaB kinase complex by TRAF6 requires a dimeric ubiquitin-conjugating enzyme complex and a unique polyubiquitin chain. *Cell.* 103:351–361. http://dx.doi.org/10.1016/S0092-8674(00)00126-4

Drees, F., A. Reilein, and W.J. Nelson. 2005. Cell-adhesion assays: fabrication of an E-cadherin substratum and isolation of lateral and Basal membrane patches. *Methods Mol. Biol.* 294:303–320.

Dynek, J.N., T. Goncharov, E.C. Dueber, A.V. Fedorova, A. Izrael-Tomasevic, L. Phu, E. Helgason, W.J. Fairbrother, K. Deshayes, D.S. Kirkpatrick, and D. Vucic. 2010. c-IAP1 and UbcH5 promote K11-linked polyubiquitination of RIP1 in TNF signalling. *EMBO J.* 29:4198–4209. http://dx.doi.org/10.1038/emboj.2010.300

Emmerich, C.H., A. Ordureau, S. Strickson, J.S. Arthur, P.G. Pedrioli, D. Komander, and P. Cohen. 2013. Activation of the canonical IKK complex by K63/M1-linked hybrid ubiquitin chains. *Proc. Natl. Acad. Sci. USA.* 110:15247–15252. http://dx.doi.org/10.1073/pnas.1314715110

Frias-Staheli, N., N.V. Giannakopoulos, M. Kikkert, S.L. Taylor, A. Bridgen, J. Paragas, J.A. Richt, R.R. Rowland, C.S. Schmaljohn, D.J. Lenschow, et al. 2007. Ovarian tumor domain-containing viral proteases evade ubiquitin- and ISG15-dependent innate immune responses. *Cell Host Microbe.* 2:404–416. http://dx.doi.org/10.1016/j.chom.2007.09.014

Ghosh, S., and M. Karin. 2002. Missing pieces in the NF-kappaB puzzle. *Cell.* 109(Supplement 1):S81–S96. http://dx.doi.org/10.1016/S0092-8674(02)00703-1

Haas, T.L., C.H. Emmerich, B. Gerlach, A.C. Schmukle, S.M. Cordier, E. Rieser, R. Feltham, J. Vince, U. Warnken, T. Wenger, et al. 2009. Recruitment of the linear ubiquitin chain assembly complex stabilizes the TNF-R1 signaling complex and is required for TNF-mediated gene induction. *Mol. Cell.* 36:831–844. http://dx.doi.org/10.1016/j.molcel.2009.10.013

Hayden, M.S., and S. Ghosh. 2012. NF-κB, the first quarter-century: remarkable progress and outstanding questions. *Genes Dev.* 26:203–234. http://dx.doi.org/10.1101/gad.183434.111

Iwai, K. 2012. Diverse ubiquitin signaling in NF-κB activation. *Trends Cell Biol.* 22:355–364. http://dx.doi.org/10.1016/j.tcb.2012.04.001

Jiang, Z., J. Ninomiya-Tsuji, Y. Qian, K. Matsumoto, and X. Li. 2002. Interleukin-1 (IL-1) receptor-associated kinase-dependent IL-1-induced signaling complexes phosphorylate TAK1 and TAB2 at the plasma membrane and activate TAK1 in the cytosol. *Mol. Cell. Biol.* 22:7158–7167. http://dx.doi.org/10.1128/MCB.22.20.7158-7167.2002

Kirisako, T., K. Kamei, S. Murata, M. Kato, H. Fukumoto, M. Kanie, S. Sano, F. Tokunaga, K. Tanaka, and K. Iwai. 2006. A ubiquitin ligase complex assembles linear polyubiquitin chains. *EMBO J.* 25:4877–4887. http://dx.doi.org/10.1038/sj.emboj.7601360

Laplantine, E., E. Fontan, J. Chiaravalli, T. Lopez, G. Lakisic, M. Véron, F. Agou, and A. Israël. 2009. NEMO specifically recognizes K63-linked poly-ubiquitin chains through a new bipartite ubiquitin-binding domain. *EMBO J.* 28:2885–2895. http://dx.doi.org/10.1038/emboj.2009.241

Li, X., M. Commane, C. Burns, K. Vithalani, Z. Cao, and G.R. Stark. 1999. Mutant cells that do not respond to interleukin-1 (IL-1) reveal a novel role for IL-1 receptor-associated kinase. *Mol. Cell. Biol.* 19:4643–4652.

Lo, Y.C., S.C. Lin, C.C. Rospigliosi, D.B. Conze, C.J. Wu, J.D. Ashwell, D. Eliezer, and H. Wu. 2009. Structural basis for recognition of diubiquitins by NEMO. *Mol. Cell.* 33:602–615. http://dx.doi.org/10.1016/j.molcel.2009.01.012

Manders, E.M.M., F.J. Verbeek, and J.A. Aten. 1993. Measurement of co-localization of objects in dual-colour confocal images. *J. Microsc.* 169:375–382. http://dx.doi.org/10.1111/j.1365-2818.1993.tb03313.x

Matsumoto, M.L., K.C. Dong, C. Yu, L. Phu, X. Gao, R.N. Hannoush, S.G. Hymowitz, D.S. Kirkpatrick, V.M. Dixit, and R.F. Kelley. 2012. Engineering and structural characterization of a linear polyubiquitin-specific antibody. *J. Mol. Biol.* 418:134–144. http://dx.doi.org/10.1016/j.jmb.2011.12.053

Ordureau, A., H. Smith, M. Windheim, M. Peggie, E. Carrick, N. Morrice, and P. Cohen. 2008. The IRAK-catalysed activation of the E3 ligase function of Pellino isoforms induces the Lys63-linked polyubiquitination of IRAK1. *Biochem. J.* 409:43–52. http://dx.doi.org/10.1042/BJ20071365

Picard, C., J.L. Casanova, and A. Puel. 2011. Infectious diseases in patients with IRAK-4, MyD88, NEMO, or IκBα deficiency. *Clin. Microbiol. Rev.* 24:490–497. http://dx.doi.org/10.1128/CMR.00001-11

Qian, H., M.P. Sheetz, and E.L. Elson. 1991. Single particle tracking. Analysis of diffusion and flow in two-dimensional systems. *Biophys. J.* 60:910–921. http://dx.doi.org/10.1016/S0006-3495(91)82125-7

Qiao, Q., C. Yang, C. Zheng, L. Fontán, L. David, X. Yu, C. Bracken, M. Rosen, A. Melnick, E.H. Egelman, and H. Wu. 2013. Structural architecture of the CARMA1/Bcl10/MALT1 signalosome: nucleation-induced

Downloaded from on June 15, 2017

Published January 20, 2014

filamentous assembly. *Mol. Cell*. 51:766–779. http://dx.doi.org/10.1016/j.molcel.2013.08.032

Rahighi, S., F. Ikeda, M. Kawasaki, M. Akutsu, N. Suzuki, R. Kato, T. Kensche, T. Uejima, S. Bloor, D. Komander, et al. 2009. Specific recognition of linear ubiquitin chains by NEMO is important for NF-kappaB activation. *Cell*. 136:1098–1109. http://dx.doi.org/10.1016/j.cell.2009.03.007

Ruland, J. 2011. Return to homeostasis: downregulation of NF-κB responses. *Nat. Immunol.* 12:709–714. http://dx.doi.org/10.1038/ni.2055

Schindelin, J., I. Arganda-Carreras, E. Frise, V. Kaynig, M. Longair, T. Pietzsch, S. Preibisch, C. Rueden, S. Saalfeld, B. Schmid, et al. 2012. Fiji: an open-source platform for biological-image analysis. *Nat. Methods*. 9:676–682. http://dx.doi.org/10.1038/nmeth.2019

Smahi, A., G. Courtois, P. Vabres, S. Yamaoka, S. Heuertz, A. Munnich, A. Israël, N.S. Heiss, S.M. Klauck, P. Kioschis, et al. 2000. Genomic rearrangement in NEMO impairs NF-kappaB activation and is a cause of incontinentia pigmenti. *Nature*. 405:466–472. http://dx.doi.org/10.1038/35013114

Sun, S.C. 2011. Non-canonical NF-κB signaling pathway. *Cell Res.* 21:71–85. http://dx.doi.org/10.1038/cr.2010.177

Tang, E.D., C.Y. Wang, Y. Xiong, and K.L. Guan. 2003. A role for NF-kappaB essential modifier/IkappaB kinase-gamma (NEMO/IKKgamma) ubiquitination in the activation of the IkappaB kinase complex by tumor necrosis factor-alpha. *J. Biol. Chem.* 278:37297–37305. http://dx.doi.org/10.1074/jbc.M303389200

Tokunaga, F., S. Sakata, Y. Saeki, Y. Satomi, T. Kirisako, K. Kamei, T. Nakagawa, M. Kato, S. Murata, S. Yamaoka, et al. 2009. Involvement of linear polyubiquitylation of NEMO in NF-kappaB activation. *Nat. Cell Biol.* 11:123–132. http://dx.doi.org/10.1038/ncb1821

Verstrepen, L., T. Bekaert, T.L. Chau, J. Tavernier, A. Chariot, and R. Beyaert. 2008. TLR-4, IL-1R and TNF-R signaling to NF-kappaB: variations on a common theme. *Cell. Mol. Life Sci.* 65:2964–2978. http://dx.doi.org/10.1007/s00018-008-8064-8

von Bernuth, H., C. Picard, Z. Jin, R. Pankla, H. Xiao, C.L. Ku, M. Chrabieh, I.B. Mustapha, P. Ghandil, Y. Camcioglu, et al. 2008. Pyogenic bacterial infections in humans with MyD88 deficiency. *Science*. 321:691–696. http://dx.doi.org/10.1126/science.1158298

Walsh, M.C., G.K. Kim, P.L. Maurizio, E.E. Molnar, and Y. Choi. 2008. TRAF6 autoubiquitination-independent activation of the NFkappaB and MAPK pathways in response to IL-1 and RANKL. *PLoS ONE*. 3:e4064. http://dx.doi.org/10.1371/journal.pone.0004064

Weil, R., K. Schwamborn, A. Alcover, C. Bessia, V. Di Bartolo, and A. Israël. 2003. Induction of the NF-kappaB cascade by recruitment of the scaffold molecule NEMO to the T cell receptor. *Immunity*. 18:13–26. http://dx.doi.org/10.1016/S1074-7613(02)00506-X

Windheim, M., M. Stafford, M. Peggie, and P. Cohen. 2008. Interleukin-1 (IL-1) induces the Lys63-linked polyubiquitination of IL-1 receptor-associated kinase 1 to facilitate NEMO binding and the activation of IkappaBalpha kinase. *Mol. Cell. Biol.* 28:1783–1791. http://dx.doi.org/10.1128/MCB.02380-06

Wu, H. 2013. Higher-order assemblies in a new paradigm of signal transduction. *Cell*. 153:287–292. http://dx.doi.org/10.1016/j.cell.2013.03.013

Wu, C.J., D.B. Conze, T. Li, S.M. Srinivasula, and J.D. Ashwell. 2006. Sensing of Lys 63-linked polyubiquitination by NEMO is a key event in NF-kappaB activation [corrected]. *Nat. Cell Biol.* 8:398–406. (published erratum appears in *Nat. Cell Biol*. 2006. 8:424) http://dx.doi.org/10.1038/ncb1384

Xu, M., B. Skaug, W. Zeng, and Z.J. Chen. 2009. A ubiquitin replacement strategy in human cells reveals distinct mechanisms of IKK activation by TNFalpha and IL-1beta. *Mol. Cell*. 36:302–314. http://dx.doi.org/10.1016/j.molcel.2009.10.002

Yamamoto, M., T. Okamoto, K. Takeda, S. Sato, H. Sanjo, S. Uematsu, T. Saitoh, N. Yamamoto, H. Sakurai, K.J. Ishii, et al. 2006. Key function for the Ubc13 E2 ubiquitin-conjugating enzyme in immune receptor signaling. *Nat. Immunol.* 7:962–970. http://dx.doi.org/10.1038/ni1367

Yamaoka, S., G. Courtois, C. Bessia, S.T. Whiteside, R. Weil, F. Agou, H.E. Kirk, R.J. Kay, and A. Israël. 1998. Complementation cloning of NEMO, a component of the IkappaB kinase complex essential for NF-kappaB activation. *Cell*. 93:1231–1240. http://dx.doi.org/10.1016/S0092-8674(00)81466-X

Zhang, S.Q., A. Kovalenko, G. Cantarella, and D. Wallach. 2000. Recruitment of the IKK signalosome to the p55 TNF receptor: RIP and A20 bind to NEMO (IKKgamma) upon receptor stimulation. *Immunity*. 12:301–311. http://dx.doi.org/10.1016/S1074-7613(00)80183-1

Downloaded from on June 15, 2017